Optical design of a 4-off-axis-unit Cassegrain ultra-high concentrator photovoltaics module with a central receiver

JUAN P. FERRER-RODRÍGUEZ,* EDUARDO F. FERNÁNDEZ, FLORENCIA ALMONACID, AND PEDRO PÉREZ-HIGUERAS

IDEA Solar Research Group, Center for Advanced Studies in Energy and Environment (CEAEMA), Universidad de Jaén, Las Lagunillas Campus, 23071 Jaén, Spain
Corresponding author: jferrer@jaen.es

Ultra-high concentrator photovoltaics (UHCPV), with concentrations higher than 1000 suns, have been pointed out by different authors as having great potential for being a cost-effective PV technology. This Letter presents a UHCPV Cassegrain-based optical design in which the sunrays are concentrated and sent from four different and independent paraboloid–hyperboloid pairs optical units onto a single central receiver. The optical design proposed has the main advantage of the achievement of ultra-high concentration ratios using relative small mirrors with similar performance values of efficiency, acceptance angle, and irradiance uniformity to other designs.   © 2016 Optical Society of America

Concentrator photovoltaic (CPV) technology presents some advantages with respect to other renewable energy ones (efficiency, etc.), however, CPV systems have to be improved in order to be a more competitive technology [1,2]. Different authors have pointed out the advantages and potential in terms of cost reduction of ultra-high CPV (UHCPV) systems with effective concentration ratios equal to or higher than 1000 suns [3]. Despite such excellent potential, different technological barriers must be eliminated at such elevated concentration levels, namely, (1) to develop solar cells with efficiencies peaking at irradiance values higher than 1000 suns [4], (2) to design a suitable cooling mechanism capable of removing the high heat power density generated by the cells [5,6], and (3) to develop optical designs able to reach UH concentration levels with an adequate optical performance [7]. This Letter is focused on this last concern.

In relation to the optical systems involved in the UHCPV, the use of Fresnel lenses seems to limit the effective concentration ratio at around 1000 suns due to the chromatic aberration

[8]. Moreover, the use of mirrors offers a promising alternative solution to get UH fluxes, since they are not limited by the chromatic aberration [9]. However, they have the disadvantage in that large mirrors are usually required [10]. Hence, they are affected by the common problems involved in the fabrication of large reflective optical devices: they are usually expensive and difficult to manufacture [11].

In this Letter, a UHCPV module based on a new optical design that concentrates sunrays from different and independent optical units onto the same single solar cell is proposed. This approach resembles telescopes based on segmented mirrors and is intended to avoid the use of large reflective optical devices. The aim is to offer an alternative optical solution to those currently being discussed in the literature in order to develop successful UHCPV systems [7]. In this work, Cassegrain-based concentrators are considered as concentrators on account of their achromatism and ultra-compactness [12,13]. Other concentrators are also based on using pairs of primary-secondary reflective elements, some of them are compact and reach and maximum performance [14]. Moreover, the design exposed in this Letter utilizes the well-known Köhler technique to produce uniform illumination on a target [15].

The proposed design is based on an adaptation of the Cassegrain concept and consists of a kind of off-axis Cassegrain design. The sunray's concentration is performed after three optical steps in each optical unit [see the two-dimensional (2D) sketch in Fig. 1]. (1) The incoming parallel sunrays reach the primary optics and are reflected on the concave paraboloid of the revolution mirror surface (primary optical element, POE). Since these rays are parallel to the paraboloid's optical axis, then they are focused toward the focus (F). (2) The convex hyperboloid of the revolution mirror surface (secondary optical element, SOE) reflects and focuses the sunrays toward its far focus (G) (it is located inside the homogenizer), since the sunrays of step 1 converge to its near focus (F). The POE and SOE are optically coupled, since both the paraboloid's focus and the near hyperboloid's focus coincide at the same three-coordinate point. (3) The sunrays of step 2 are refracted by the homogenizer (tertiary optical element, TOE) and spread on the cell's
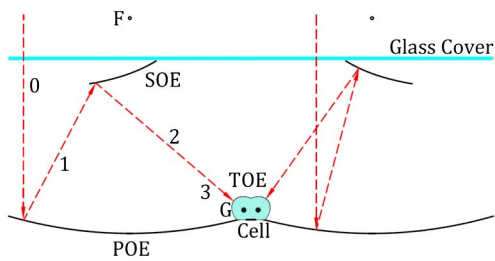
Fig. 1. Two-dimensional sketch of the rays' paths for the transverse section of two optical units through a module's diagonal. (0) Incoming sunrays; (1) reflected rays on the primary optics; (2) reflected rays on the secondary optics; (3) rays transmitted through the tertiary optics and impinging the solar cell. The foci of the two-sheeted circular hyperboloid are (F) and (G), where (F) is also the circular paraboloid's focus.

surface. The homogenizer's optical active surface is a Cartesian oval of revolution optically coupled to the hyperboloid mirror.

The module presented in this Letter is composed of four symmetrical and independent optical units (see Fig. 2) with the axis of symmetry being normal through the center of the solar cell's plane. Each optical unit is based on the adaptation of the Cassegrain design described above (see Fig. 1) and consists of a set of three optical elements: one square paraboloid mirror (POE), one trimmed (resulting in four edges) hyperboloid mirror (SOE), and one Cartesian oval of revolution (TOE). The homogenizer is the assembly of the four Cartesian ovals of revolution (one for each optical unit) and functions as a Köhler integrator, thus, it contributes to spreading out the sunrays onto the solar cell [16] [as it is shown in Fig. 2(b)]. Each Cartesian oval of revolution couples the more external vertex of each secondary mirror with each vertex of the opposite side of
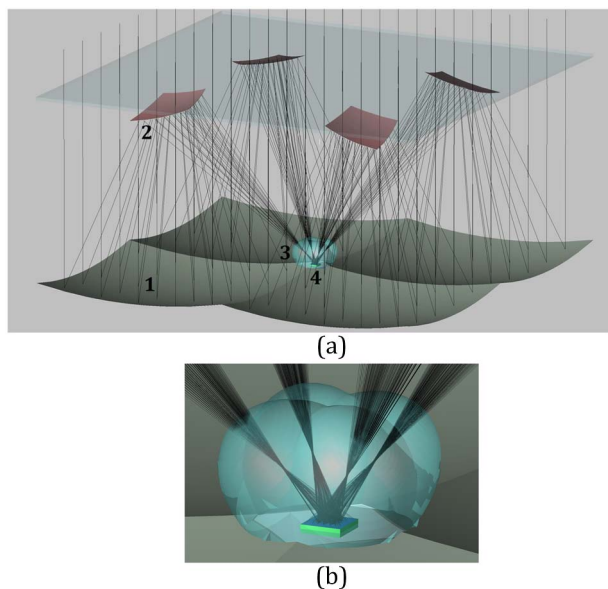
Fig. 2. (a) Model and ray tracing of the Cassegrain 4-optical-unit module with the central receiver. The elements are marked: (1) paraboloid mirrors (POE), (2) hyperboloid mirrors (SOE), (3) homogenizer (TOE), and (4) solar cell. (b) Detail of ray tracing at the central receiver.

the solar cell [17]. In more detail, each POE mirror is based on a circular paraboloid described as

$$\frac{x^2}{24.5^2} + \frac{y^2}{24.5^2} - z = 0. \tag{1}$$

Whereas each secondary mirror is based on the open upwards sheet of a two-sheeted circular hyperboloid, which can be described as

$$\frac{x^2}{64.5^2} + \frac{y^2}{64.5^2} - \frac{z^2}{42.5^2} = -1, \tag{2}$$

where x, y, and z are in millimeters. In the case of the design proposed, the SOE's shape has been trimmed by the contour of the light beam that impinges its reflecting surface. The shape of each Cartesian oval of revolution has as the generatrix curve as the locus resulting after solving the differential equation of conservation of the optical path length of any ray trajectory between a vertex of the solar cell and the opposite vertex of the correspondent secondary mirror. The generatrix curve is then revolved around the axis defined between the two vertexes. The height of each individual solid Cartesian oval of revolution along its longitudinal axis is chosen to be 20 mm from its basis—the basis matches the correspondent solar cell vertex. The location of the far focus of the SOE mirror has as relative positive Cartesian coordinates, with respect to the solar cell surface's center (which is 10 mm over the plane, defined by the centers of the POE mirrors), the next values: $(x, y, z) = (3.54, 6, 3.54)$ mm. The module has symmetry around the normal at the solar cell's center in steps of 90°, i.e., each of the four optical units corresponds to an identical quadrant portion of the module. For the simulations, a glass frontal exterior covering, needed to protect the module against soiling, water, etc., is also included. The SOE mirrors can be fixed to the interior side of the glass covering by adding a small support like a cylinder.

The geometrical concentration ratio is $C_g = 2304X$, since the cell is of 5 × mm × 5 mm and each paraboloid mirror is of 120 × mm × 120 mm. Each paraboloid is of 150 mm focal distance. For each hyperboloid, the far focus is at 120 mm in front of the mirror (front focal distance) and the near focus is 35 mm back from the mirror (back focal distance). The module has a depth of 123 mm.

The optical simulation was performed by simulating the solar ray's source, taking into account the solar angular profile (4.65 mrad) and also, the solar spectral distribution of energy (for simplicity, extra-terrestrial spectrum ASTM E-490-00). For both optical design and simulations, the software TracePro was used. Figure 2 shows the ray tracing and the sunray's concentration from the four different optical units to the same target. The planar frontal glass covering is simulated as fused silica. All the mirrors have been simulated as "standard mirror" in TracePro. It corresponds to a surface with the next flux coefficients: absorptance = 0.05, specular reflectivity = 0.949, and integrated bidirectional reflectance distribution function (BRDF) = 0.001324 using the ABg scatter model. The homogenizer is simulated as if made of B270 glass and the solar cell as the perfect absorber.

From the optical simulation, the optical efficiency of this design, defined as the ratio between the power reaching the solar cell over the module's incoming power, results $\eta = 73\%$, resulting an effective concentration ratio of 1682 suns. If the

glass covering is not considered, the calculation of the efficiency increases up to 79%. The 3D irradiance map on the cell is not completely uniform and has a relative small "hole" (less irradiance in the cell's center than in its surroundings, see Fig. 3). The irradiance distribution on the solar cell reaches a maximum of 5480 suns and has an average value of 1682 suns; when simulating an incoming power of 1000 W/m²–the maximum value is around 3.3 times higher than the average one. Each of the four rays' beams is impinging on the solar cell with an average angle of approximately 30° with respect to the normal at the solar cell's surface.

In Fig. 4, the effective acceptance angle characteristic (considering the finite angular aperture of the sun) of the whole optical system is presented. The relative transmission efficiency of 0.9 (relative to the maximum optical efficiency value) corresponds to a misalignment angle of 0.61°. From this value, the effective concentration-acceptance angle product (CAP*) can be calculated, resulting 0.51.

The summary of the simulation results of this 4-optical-unit design module and its geometrical parameters are presented in Table 1.

The values shown in Table 1 are similar compared to the optical performance results of other Cassegrain designs [18–22] for which the optical efficiency ranges from 0.62 [18] to 0.85 [21], CAP* values vary from 0.36 [18] to 0.47 [21], and the geometrical concentration ratio is between 500× [21] and
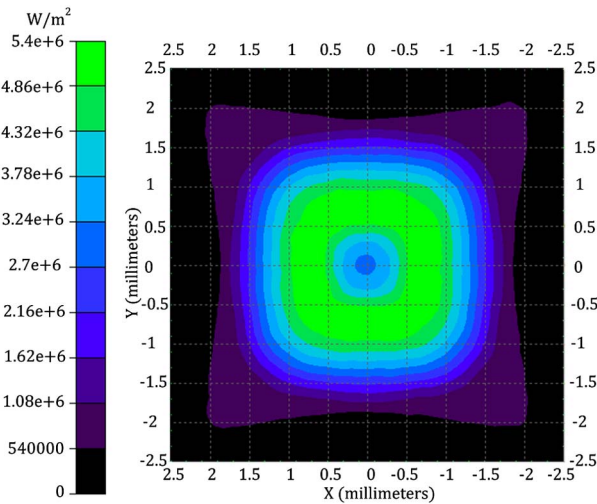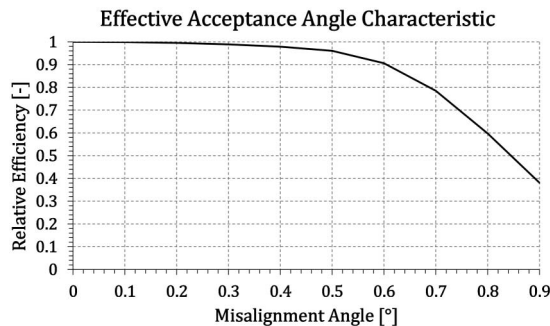
Table 1. Summary of Geometrical and Simulation Parameters

Magnitude	Value
Geometrical Concentration Ratio [–]	2304
Optical Efficiency [–]	0.73
Effective Concentration [suns]	1682
Effective Acceptance Angle [°]	0.61
Effective Concentration-Angle Product [–]	0.51
Optical Efficiency without Glass Covering [–]	0.79
Cell's Irradiance Maximum [suns]	5480
Cell's Irradiance Maximum over Average [–]	3.3

1057× [19]—much lower than in the design proposed. In relation to the irradiance distribution over the solar cell, the two best designs, among the above cited ones, are a two-mirror Köhler-based design with a cell's irradiance maximum over average value near to 2.6 [22], and a Cassegrain-based design with a kaleidoscope homogenizer with a value near to 1.4 [21].

Concerning the optical efficiency of the design, the global optical efficiency losses are explained in terms of the next factors: (1) transmission through the planar frontal glass covering, (2) the shadow of the SOE and (3) TOE, (4) the metallic reflection on the POE and (5) SOE, and (6) the transmission through the TOE. For each loss factor, an optical efficiency, η_i, and the associated optical losses, Losses$_i$ = 1 − η_i, can be defined. The global optical efficiency, η_{global}, can be expressed as

$$\eta_{\text{global}} = \prod_{i=1}^{i=6} \eta_i = 0.73, \tag{3}$$

where $i = 1$ to 6 corresponds to each loss factor item in Table 2. The global losses can be calculated as Losses$_{\text{global}}$ = 1 − η_{global} = 0.27. The correspondent optical efficiencies for each loss factor, and the associated optical losses, are listed in Table 2.

Both the SOE and TOE shadowing are shrinkable. Reducing the near focal distance of each SOE, the useful mirror area will decrease. Nevertheless, due to the conservation of the étendue, the sunrays' focalization at the SOE's far focus will be worse, and this has to be considered as a trade-off between both characteristics. Concerning the TOE shadowing, the size of each Cartesian oval of revolution can be reduced in the trade-off with the acceptance angle characteristic of the module.

It is important to note that, although the proposed design may be relatively complex due to the relatively high number of optical elements needed, it offers some important opportunities. This design is a way of reaching UH concentration ratios

Fig. 3. Irradiance map of the incident rays on the solar cell.

Fig. 4. Effective acceptance angle characteristics of the design.

Table 2. Detailed List of Optical Losses

	Optical Efficiency [–]	Optical Losses [%]
1. Glass Cover Transmission	0.931	6.9
2. SOE Shadowing	0.925	7.5
3. TOE Shadowing	0.991	0.9
4. POE Reflectance	0.949	5.1
5. SOE Reflectance	0.949	5.1
6. TOE Transmission	0.955	4.5
Global	0.73	27

while avoiding the use of large concentrating mirrors which are, apparently, more expensive and difficult to fabricate than smaller ones, as previously stated [10,11]. Moreover, the height of the POE is reduced 75% (36 mm) when compared with having only one single parabolic mirror of the same focal distance. Furthermore, since the POE and SOE are quadric surfaces, they may be easier to be manufactured, in general, than freeform surfaces if these last do not have a symmetry axis [23]. Another opportunity of this design is derived from the use of a Köhler-based homogenizer, which provides more degrees of freedom in the optical design.

In analyzing the compactness of this design, the more compact this design is the higher the incident angle of rays over the cell, and therefore, Fresnel losses on the cell are higher. However, the relative low rays' incident angle on the solar cell's plane is a guarantee of not having significant Fresnel reflecting losses at the solar cell's surface [24]. Another limitation is related to the conservation of the étendue, since it contributes to spread out the concentrated sunrays. This is more evident if the design is tuned to reduce the size of the SOE mirrors in order to decrease the shadowing losses.

Considering the maximum concentration value over the solar cell (see Fig. 3), it does not represent a problem for up-to-date HCPV solar cells in terms of their reliability which some authors demonstrated by measuring triple-junction cells at very high concentration ratios, even up to around 1×10^4 suns [25]. The maximum irradiance value of the proposed design results in less than four times the average irradiance on the solar cell, a value that is slightly higher than other designs, as it was mentioned above. This value should be improved in future designs, since it may have an impact on the fill factor of the solar cell's I–V curve, and therefore, reduce the efficiency of the whole concentrator module [26]. As can be seen in Fig. 3, the irradiance pattern on the cell's surface has a 90° step symmetry, since the four irradiance patterns of the four optical units are summed on the solar cell's surface. The impact of the shadow of each SOE on the total irradiance distribution leads to a central region with lower values than its surroundings [16].

In order to improve the optical performance of this design, different variations of primary and secondary mirrors' focal distances can be explored. Also, the calculation of the homogenizer can be varied, due to the degrees of freedom existing in the design, in searching for an improvement of both irradiance uniformity and acceptance angle.

In conclusion, a new UHCPV (i.e., effective concentration higher than 1000 suns) module design based on the Cassegrain design (pair paraboloid–hyperboloid) with four optical units around a central receiver has been designed. Each one of these optical units is an adaptation of the conventional Cassegrain design in order to send the sunrays out of the axis defined by the paraboloid mirrors (primary optics). The effective CAP* of the design is relatively good at 0.51 with an effective acceptance angle of 0.61°. The optical efficiency is 73%, the geometrical concentration ratio is 2304×, and the effective concentration value is 1682 suns. Without considering the covering glass, the optical efficiency is 79%. These simulation results assure the optical feasibility of the design concept implemented in this Letter. The UHCPV module's proposed optical design represents a good trade-off between the acceptance angle and irradiance uniformity, having similar optical performance values to other designs, while avoiding the use of relatively large concentrating mirrors.

REFERENCES

1. P. Pérez-Higueras and E. F. Fernández, *High Concentrator Photovoltaics: Fundamentals, Engineering and Power Plants* (Springer, 2015).
2. D. Talavera, P. Pérez-Higueras, J. Ruíz-Arias, and E. F. Fernández, Appl. Energy **151**, 49 (2015).
3. C. Algora and I. Rey-Stolle, in *Next Generation of Photovoltaics* (Springer, 2012), pp. 23–60.
4. E. F. Fernández, A. García-Loureiro, and G. Smestad, in *High Concentrator Photovoltaics: Fundamentals, Engineering and Power Plants* (Springer, 2015), pp. 9–37.
5. L. Micheli, E. F. Fernández, F. Almonacid, K. Reddy, and T. Mallick, AIP Conf. Proc. **1679**, 130003 (2015).
6. L. Micheli, E. F. Fernández, F. Almonacid, K. Reddy, and T. Mallick, in *42nd IEEE Photovoltaic Specialist Conference (PVSC)* (IEEE, 2015), pp. 1–6.
7. K. Shanks, S. Senthilarasu, and T. K. Mallick, Renewable Sustainable Energy Rev. **60**, 394 (2016).
8. F. Languy, K. Fleury, C. Lenaeerts, J. Loicq, D. Regaert, and T. Thibert, Opt. Express **19**, A280 (2011).
9. K. Shanks, S. Senthilarasu, and T. Mallick, in *High Concentrator Photovoltaics: Fundamentals, Engineering and Power Plants* (Springer, 2015), pp. 85–113.
10. K. Lovegrove, G. Burgess, and J. Pye, Sol. Energy **85**, 620 (2011).
11. D. Malacara and B. J. Thomsom, *Handbook of Optical Engineering* (CRC Press, 2001).
12. R. Winston and J. M. Gordon, Opt. Lett. **30**, 2617 (2005).
13. K. Shanks, N. Sarmah, J. P. Ferrer-Rodriguez, S. Senthilarasu, K. S. Reddy, E. F. Fernández, and T. Mallick, Sol. Energy **131**, 235 (2016).
14. A. Goldstein, D. Feuermann, G. Conley, and J. Gordon, Opt. Lett. **36**, 2836 (2011).
15. R. Wiston, J. Miñano, and P. Benítez, *Nonimaging Optics* (Elsevier, 2005).
16. R. Winston and W. Zhang, AIP Conf. Proc. **1407**, 105 (2011).
17. M. Hernandez, A. Cvetkovic, P. Benitez, and J. Minano, Proc. SPIE **7059**, 705908 (2008).
18. C. Liang and J. Lin, Sol. Energy **122**, 264 (2015).
19. M. Dreger, M. Wiesenfarth, A. Kisser, T. Schmid, and A. Bett, in *Proceedings of CPV-10 Conference* (2014), Vol. **177**.
20. P. Benitez, A. Cvetkovic, R. Winston, L. Reed, J. Cisneros, A. Tovar, A. Ritschel, and J. Wright, in *Conference Record of the 2006 IEEE 4th World Conference on Photovoltaic Energy Conversion* (IEEE, 2006), pp. 690–693.
21. K. Shanks, N. Sarmah, K. Reddy, and T. Mallick, AIP Conf. Proc. **1616**, 211 (2014).
22. R. Winston, P. Benitez, and A. Cvetkovic, Proc. SPIE **6342**, 634213 (2006).
23. M. Nijkerk, O. Van der Togt-Marinescu, and G. Gubbels, "Freeform design and fabrication : where the proof of the pudding is in verification," in *International Conference on Space Optics*, Rhodes, Greece, 2010.
24. A. Bäuerle, A. Bruneton, J. Wester, J. Stollenwerk, and P. Loosen, Opt. Express **20**, 14477 (2012).
25. J. Gordon, E. Katz, D. Feuermann, and M. Huleihil, Appl. Phys. Lett. **84**, 3642 (2004).
26. H. Baig, K. Heasman, and T. Mallick, Renewable Sustainable Energy Rev. **16**, 5890 (2012).